ESS Detector Strategy for LoKI (DRAFT)

K. Kanaki [*1], R. Hall-Wilton [†1,2], A. Jackson [‡1,3], and S. Kolya [§1]

[1]*European Spallation Source (ESS AB), P.O. Box 176, SE-22100 Lund, Sweden*
[2]*Mid-Sweden University, SE-85170 Sundsvall, Sweden*
[3]*Physical Chemistry, Lund University, P.O. Box 124, SE-22100 Lund Sweden*

September 12, 2014

1 The LoKI instrument at ESS (DRAFT)

The peak brightness of ESS will be higher than that of any of the existing pulsed sources, and it will be more than one order of magnitude higher than that of the ILL, the world's leading continuous source [**?**].

According to the current status, the ESS instrument suite will include two SANS instruments with LoKI being the first one endorsed for tranche 1 in late 2019 and having already entered the preliminary design phase (Phase 1). This document is one in a list of documents necessary for Phase 1 and it serves as material for the LoKI STAP review in September 2014. It will address the appropriate detector technology solutions and decision points for LoKI, their maturity and cost, and it will put together a realization time schedule including decision milestones towards 2019.

The requirements that pose the biggest challenge on the detector choices for LoKI are high rate capability and cost due to the large surface coverage foreseen. The area the LoKI detectors cover, as described in the geometry considerations of the proposal [**?**], is divided in zero-, low- and high-angle regions, in order to address the requirements in a more efficient way and as a function of polar angle. Zero-angle includes beam and transmission monitors, low-angle is the rear detector (the ^{3}He detector in a traditional SANS configuration) that will cover the low Q region and high-angle includes either the 'barrel' detector or two big window frame panels that are closest to the sample.

In addition to the high rate capability, position information is required, which means that the spatial resolution plays a role in the technology and geometry choice. In the following sections, the detector requirements for LoKI are defined and quantified, where possible, given the current status of the performance analysis. This document is work in progress.

2 Definition of detector requirements

Apart from the more technical requirements that usually characterize the performance of a detector, it is essential to look at the wider picture, meaning that an evaluation of the scientific performance of the detector within the whole instrument has to be conducted. However, for Phase 1 not all aspects of such a performance need to be addressed. A generic list of detector requirements for LoKI could look like the following:

Main Detectors

- Spatial/angular resolution: how well the neutron position is measured. It impacts the λ and Q resolution.

[*]kalliopi.kanaki@esss.se
[†]richard.hall-wilton@esss.se
[‡]andrew.jackson@esss.se
[§]Scott.Kolya@esss.se

- Time resolution: how well the time of flight (arrival time at detection point/pixel) is measured.
- Efficiency: the fraction of neutrons detected compared to the true number of neutrons hitting the same area.
- Global rate (Hz): the total counting rate the entire detector is exposed to.
- Local rate (Hz/cm^2 or Hz/mm^2): the rate, defined over a smaller area of a cm^2 or a mm^2, a channel or a pixel.
- Local instantaneous rate: hits during a small interval of time over a smaller area (channel or pixel), hits/μs-ms/mm^2.
- Dynamic range: the smallest and highest values of the signal that can be detected above the noise.
- Signal/Background (S/B ratio): the ratio of the signal events over everything else that is not signal-related. The background sources are several, various and need special attention.
  - natural background signal from the detector and its electronics.
  - gamma rays from the neutron conversion process, cosmics, prompt pulse, sky-shine, ground-shine
  - fast neutrons stemming from the prompt pulse, sky-shine, ground-shine
  - cosmics
  - natural activity from surrounding materials
  - background from neighbouring instruments during measurements
  - scattering of neutrons on the detector materials giving rise to fake signals
  - incoherent and inelastic scattering that is of no interest for the science case
- Calibration and alignment: how well the measured quantities are known.

Beam and transmission monitors

- Ability to characterize the neutron beam in terms of wavelength distribution and flux.
- Ability to normalize the Q distribution (per pulse?).
- Ability to reconstruct the shape of the beam profile.

Note that in this document only the most difficult requirements are addressed in detail. In addition these definitions are in the process of rigorous definition and they will be described in detail in a separate dedicated document that is in preparation by the ESS Detector Group.

3 Possible Detector Geometries for LoKI: preliminary considerations

As presented in the instrument proposal, two detector geometries are chosen for the preliminary performance study that will help define and refine the detector requirements. The proposed geometries are not considered binding but should serve as a starting platform for the optimization. The two geometries shown in Figure 1 look at first glance wildly different; however from the point of view of detectors the main choices (in terms of eventual scientific performance) are similar.

The feature that the two geometries share at the moment is a small rear detector covering low scattering angles and populating the low Q regime. This detector will be referred to as 'low-angle' detector from now on. Both geometries will also make use of a transmission monitor that will be referred to as 'zero-angle' detector in the coming sections. The two largest panels of the window frame configuration or the alternate polygonal 'barrel' detector, cover larger scattering angles and will be referred to as 'high-angle' detector. Note that the latter dominates the geometrical differences in Figure 1. It also implies very different conditions/costs for the vacuum flight tank.

Starting from these geometries as conceived at the moment, a preliminary performance evaluation of the detectors (see Appendix) can help quantify the major requirements for achieving the goals of Phase 1. The latter are summarized in Table 1.

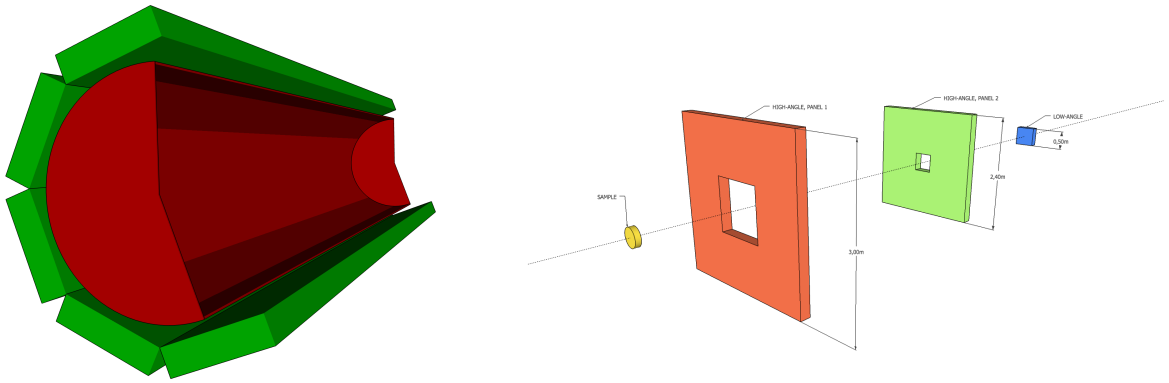

(a) (b)

Figure 1: Possible detector geometry configurations for LoKI, as they appear in the instrument proposal. Figure 1a depicts the 'barrel'-like arrangement, while Figure 1b shows the window frame geometry.

	active area	θ coverage	spatial resolution	time resolution	local rates
zero-angle	~70 cm^2	0°-0.5°	sub-mm ??	μs	9×10^8 Hz/cm^2
low-angle	0.25-1 m^2	0.5°-4°	3 mm	μs	500 Hz/mm^2(S), <70 Hz/mm^2(W)
high-angle (WF)					
mid-panel	6 m^2	4°-27°	0.5-1 cm	μs	140 Hz/cm^2(S), 1.3 kHz/cm^2(W)
front-panel	8 m^2	27°-56°	1-3 cm	μs	3 Hz/cm^2(S), <5 kHz/cm^2(W)
high-angle (B)	16-34 m^2	3°-90°	1-3 cm	μs	<3 kHz/θϕ bin (S), 3 kHz/θϕ bin (W)

Table 1: Preliminary detector requirements for the window-frame (WF) and 'barrel' (B) configurations. (S) stands for spheres (200 Å) and (W) for a water sample. The rear detector is placed at 5.5 m and a collimation of 2 m has been used to emulate the worst case scenario conditions.

4 State of the art: what is possible with today's technologies

^{3}He is by far the most commonly used technology today with a few exceptions where scintillators are preferred. An overview of the main instruments operated around the world is presented in Table 2. The SANS instruments are dominated by ^{3}He detectors in various shapes, e.g. 8 mm thick tubes, Multi-Wire Proportional Counters (Ordela) or in single cylindrical volumes with multiple anode wires.

instrument@ facility	detector technology	area (cm×cm)	spatial resolution (mm×mm)	global rate
Loq@ISIS	^{3}He-CF_4/Ordela, 4×ZnS	64×64	5-10×5-10, 12×12	-
SANS2d@ISIS	^{3}He-CF_4??? (×2)	96.5×96.5	5×5	-
ZOOM@ISIS	^{3}He	100×	8×	-
Larmor@ISIS	^{3}He	60×60	8×8	-
EQ-SANS@SNS	^{3}He	100×100	8×7	-
TAIKAN@J-Parc	^{3}He/window frame	-	8 ?	-
SANS-I@PSI	^{3}He	96×96	7.5×7.5	-
SANS-II@PSI	^{3}He (circular)	64(R)×55	4.3 (0.2-0.7*SANS-I)	90 kHz (11.3 µs)
D11@ILL	^{3}He	96×96	7.5×7.5	2.4 MHz (420 ns)
D22@ILL	^{3}He	102.4×98	8×8	5 MHz (2 µs?)
D33@ILL	^{3}He/window frame	64×64, 4 16×64	5×5	-
D17@ILL	^{3}He/monoblock tube	30×48	1.2×7.6	0.75 MHz
Quokka@ANSTO	^{3}He	100×100	5×5	-
Bilby@ANSTO	^{3}He/window frame	64×64, 32×64	8×	-
NG3 30m@NIST	^{3}He/Ordela	64×64	5.08×5.08	30 kHz
NG7@NIST	^{3}He/Ordela	64×64	5.08×5.08	-
NG5 10m@NIST	^{3}He	64×64	5.08×5.08	-
NG6 VSANS 10m@NIST	^{3}He/window frame	64×64	8 mm	11 MHz
KWS-1@FRM-II	Anger camera	60×60	5.3×5.3	0.6 MHz
KWS-2@FRM-II	Anger camera high res. scintillator	60×60 diameter=8.7	5.25×5.25 0.45×0.45	0.6 MHz -
KWS-3@FRM-II	-	-	-	-
SANS-1@FRM-II	^{3}He	100×100, 50×50	8×8, 3×3	-

Table 2: Detector features on SANS instruments at existing facilities, where figures are publicly available. The most popular instruments are highlighted in boldface font. The ones that are under construction/commissioning appear in italic font. The facility order is random. Rates and efficiency are not always readily available.

4.1 ^{3}He Detectors

So far the choice for ^{3}He detector being the default was based on the high neutron absorption cross section of the isotope leading to high detection efficiency, the good γ discrimination capability and the (pre-2009) reasonable total cost of the detector. Also the position resolution of 8 mm and the rate capabilities suited the intensities of the available neutron sources in the world. As today's 'golden standard' for SANS detectors it is worthwhile to quantify its performance.

The neutron detection efficiency is traditionally purely quoted solely in terms of the ^{3}He path length (i.e. bar-cm) that a neutron crossing the centre of a tube sees; other design related effects are explored in this section. Note that none of the neutron efficiency performance numbers quoted in this section relate to a specific instrument. They are however broadly and qualitatively representative of the design and engineering choices made in current SANS instruments.

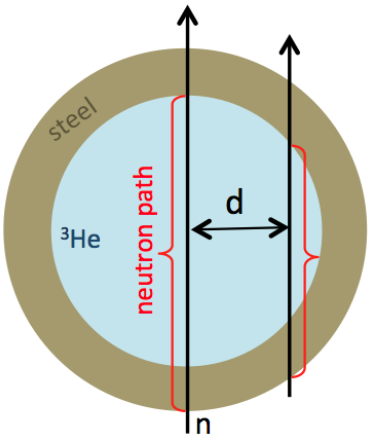

Figure 2: Definition of the distance parameter as used in the detector efficiency calculations.

As mentioned before, 8 mm diameter ^{3}He tubes are the standard detector choice in today's SANS instruments. They are typically operated in high pressure and the stainless steel walls that encase the converting-counting gas have a typical thickness of 0.5-1 mm. Given the simplicity of the geometry it is possible to analytically evaluate the efficiency of such a tube including the impact of the detector tube walls and the Cd foils used between the tubes to reduce the number of fake events due to scattering. Again for simplicity, when considering interactions in the detector tube walls, neutron absorbed and half of those incoherently scattered are considered as undetected.

Figure 3 depicts such an analytical evaluation for an 8 mm thick ^{3}He tube in a steel case of 1 mm thickness. The efficiency of the ^{3}He tube is presented as a function of the total neutron path inside the detector for a variety of neutron wavelengths for a gas pressure of 10 bar. The neutron path

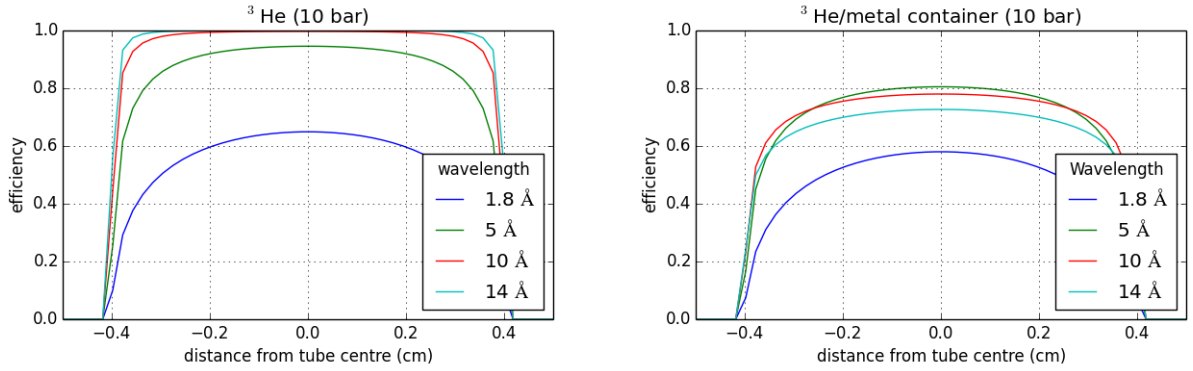

(a) (b)

Figure 3: ^{3}He gas efficiency vs. distance from the center of an 8 mm tube for a selection of wavelengths (see 3a). Same calculations repeated including 1 mm thick steel walls (see 3b).

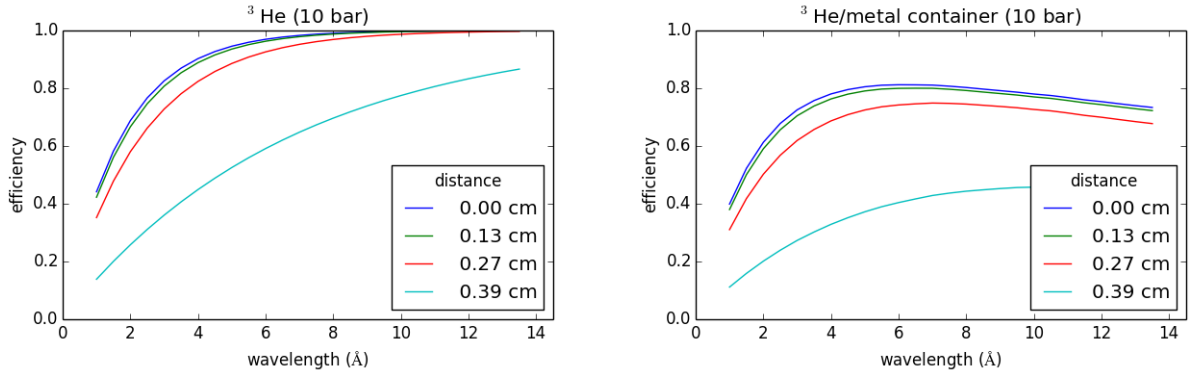

(a) (b)

Figure 4: ^{3}He gas efficiency vs. wavelength for a selection of distances from the center of the ^{3}He tube (see 4a). Same calculations repeated including the impact of the steel walls (see 4b).

is represented by the distance of the neutron track from the center of the tube as defined in Figure 2. No angular dependence has been considered for these calculations, as the detectors are placed several meters away from the sample. The neutrons are assumed to always hit the tube perpendicularly. The counting gas is pure ^{3}He. The detection process is assumed to be perfect. Alternatively, the same efficiency can be plotted as a function of wavelength as depicted in Figure 4. In both Figures, 3 and 4, the plots at the central position represent the efficiency figures traditionally quoted for ^{3}He.

So far the efficiency of a single tube has been considered. If we include the effects of the Cd foils placed between the detector tubes and study the impact thereof on the total geometrical acceptance of the detector setup, we find that the foils effectively scale the efficiency further down. Assuming a typical Cd foil thickness of 0.5-1 mm, by simple geometrical considerations in the case of 8 mm tubes, it turns out that there is an additional reduction effect of about 5-10%. a rather small effect for the particular geometry. Also, considering the assembly of the single tubes into groups of e.g. 100 units, as is often done in real instruments, it is necessary to further account for the loss of geometrical acceptance in the average efficiency. The sum of these effects is presented in Figure 5. In total, the reduction amounts to about a factor 0.9-0.95. The impact of any entrance window or of threshold effects due to charge division has not been evaluated here.

The plots shown in Figure 5 are representative of the effects that need to be considered in the design. The efficiencies in Figure 5 can be considered as the detection efficiency of a neutron from the sample entering the solid angle subtended by the detector system towards the sample. This can be seen as representative of the appropriate efficiency given by the state of the art detectors for present detectors in SANS instruments.

This is particularly pertinent here, for the design of detectors for such applications at ESS, as with

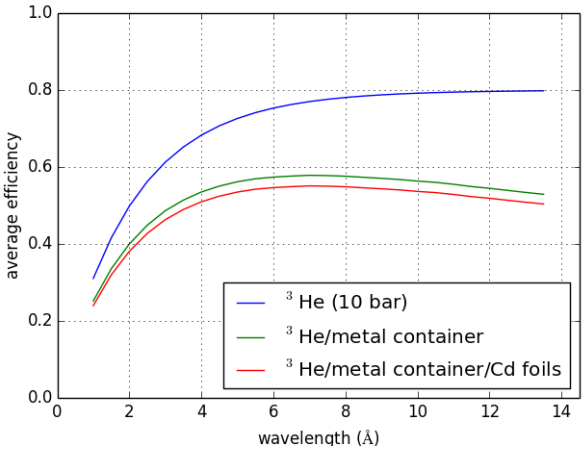

Figure 5: Average efficiency of an 8 mm thick ^{3}He tube as a function of neutron wavelength including the wall effects and the reduction in geometrical acceptance from the Cd foils and the assembly of the tubes.

the new technologies, these compromises in the engineering design will differ. Therefore, this definition of efficiency is the one that is more appropriate for comparison between different technology choices, as it is the efficiency which more closely represents the effect on the eventual instrument performance.

In terms of counting rate capability, neutron detection efficiency and γ-ray sensitivity, ^{3}He is a superior technology to scintillators. Most existing SANS instruments, summarised in Table 2 use this technology. Gaseous detector have several designs and performances, typically for cold neutrons (2.5-30Å), ^{3}He detectors have efficiencies of 50–90%, global count rates of 20 kHz-30 MHz, and local count rates of 200–300 Hz/mm^2. The requirements of the LoKI detectors are above what the best ^{3}He detectors can do at the moment, so this solution is not worth considering. In addition the extreme cost of these detectors would decimate the instrument budget.

4.2 Scintillators

Scintillators available and mostly used are ^{6}LiF/ZnS(Ag) [**?**] and GS20 [**?**] (Lithium glass). The neutron detection efficiency for scintillators varies between 40% and 75% for 2.5 Å, which is slightly lower than standard ^{3}He tubes. The spatial resolution that can be achieved with scintillators in Anger camera type [**?**], [**?**] or WLS fibre readout [**?**], [**?**], [**?**] detectors is below 1 mm and few mm respectively and fulfil the ESS requirements for the low-angle area of LoKI.

From Table 2 it becomes apparent that among the major facilities in the world, it is only FRM-II SANS instruments (KWS-1, KWS-2, KWS-3) that have adopted scintillator technology. Their resolution requirements are similar, if not looser, compared to LoKI. In terms of rates, the flux on sample at these beamlines is smaller than at the ESS. The global count rates cited for the KWS instruments are 600 kHz. However, 100 kHz is the maximum count rate limit for scintillators coupled with a PMT, which can at best reach the same counting rate capability as ^{3}He, which poses a limitation for use on LoKI.

Uniformity of count along the detector surface is claimed to be in between the 10% variation. Local counting rate capability is about 400 Hz/mm^2, which is similar to the fastest existing ^{3}He detectors. The predicted rates for LoKI are higher, which means a significant effort is required to match these requirements.

5 Strategy for selection of suitable detector technologies

The requirements for the LoKI detectors display a strong dependence on the scattering angle and the division of the polar angle space in three distinct regions is intended to facilitate the evaluation and the technology decision. Thus, for formulating the decision making strategy we will follow the same structure. In this section only the detector developments that can serve the LoKI needs are mentioned.

5.1 Zero-angle detector (0°-0.5°)

Zero-angle detectors include the beam monitors used along the neutron guides for beam diagnostics and the transmission monitors installed after the sample. They are low efficiency detectors for flux measurements and data corrections. The most critical requirements for such a detector are the rate capability, stability and radiation hardness. It should withstand neutron fluxes of the order of $10^9/\mathrm{cm}^2/\mathrm{s}$ in LoKI's case and its performance should not degrade for an acceptable period of time. The rate requirements will be higher for the monitors placed after the choppers for diagnostics purposes. The evaluation of the time resolution and efficiency requirements is on-going and will become more detailed within Phase 2. The beam monitors and to a certain extent the transmission monitors are expected to be similar across the ESS suite.

Suitable technologies for the zero-angle detectors are:

- Low pressure gaseous detectors
- Scintillators (ISIS)
- Semiconductor detectors [**?**], [**?**]
- Fission chambers
- Micromegas

5.2 Low-angle detector (0.5°-2°/4°)

The low-angle detector presents the biggest challenge in terms of rate and spatial resolution. Suitable technologies that fulfil the requirements are briefly described in the following sections.

- Multi-Blade [**?**], [**?**]
- Micro-Pattern Gaseous Detectors (MPGD) [**?**], [**?**], [**?**]
- A1-CLD
- Scintillators/SoNDe
- ^{3}He detectors

5.2.1 Multi-Blade

Due to the mm-range spatial resolution requirements of LoKI only inclined geometry detectors are considered here. The ILL designed Multi-Blade prototype [**?**] is a small area detector that can be scaled up to fit the size needs of the low- and high-angle detector banks. It is a Multi Wire Proportional Chamber (MWPC) operated at atmospheric pressure. The Multi-Blade prototype (see figure 6) uses $^{10}B_4C$ [**?**] converters at small grazing angle (∼5°).

Thanks to the inclined geometry, the Multi-Blade prototype can reach counting rates up to about 10 times larger than ^{3}He capability tubes at present (it would be about 2 kHz/mm^2). It has been shown that its neutron detection efficiency can be above 40% at 2.5 Å, similar to detectors used presently. The detector is operated at atmospheric pressure in a continuous gas flow.

Due to these advantages, the Multi-Blade design is one of the favoured development paths to be pursued for LoKI. In terms of recent overviews of the R&D status of the ^{10}B Multi-Blade design, please see [**?**, **?**, **?**].

When neutron scattering is performed on soft matter samples, the incoherent scattering from hydrogen atoms gives a significant contribution to the total scattering signal. Single layers of the multi-layer boron based detector have neutron conversion efficiency, which is strongly dependent on the wavelength of the neutron. Therefore the depth of the interaction of the neutron with several layers in a detector carries statistical information about the energy of the detected neutron. In case of sufficiently high statistics, this provides a coarse energy resolution, which can discriminate against this inelastic scattering. These developments are at their outset, however, may mature sufficiently to be implemented for detector geometries where there is more than one interaction layer.

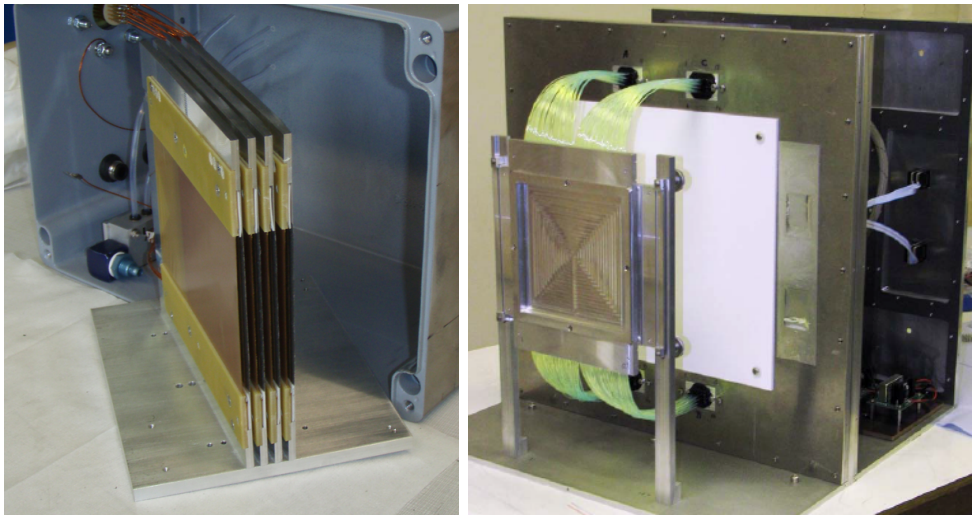

Figure 6: The Multi-Blade prototype developed at ILL (left). The WLS scintillating detector developed at ISIS (right).

5.2.2 Micro-Pattern Gaseous Detectors (MPGD)

The Micro-pattern gaseous detectors (MPGD) [**?**] family includes Micro-Strip Gas Chambers (MSGC), Gaseous Electron Multipliers (GEM), and Micromegas. In general these detectors offer intrinsic high rate capability ($\sim$1 MHz/mm^2) with excellent spatial resolution ($<$30 μm) [**?**]. These detectors are very widely used: from high energy physics, to space science (many MSGCs are used in satellites), to underground laboratories and beyond. In neutron scattering, the best known applications are the ^{3}He MSGC installed on D20, and the ^{10}B based CASCADE detectors [**?**], installed at the RESEDA instrument at FRM-II.

Given their intrinsic rate and resolution capabilities, this technology is an obvious candidate for the low-angle region of LoKI. Technically this is not a detector category by itself but rather a variation on the Multi-Blade technology under development.

In order to increase the counting rate capability, the readout system can be replaced by GEMs. There is no question as to the rate or resolution possible from such detectors, which exceeds the requirements necessary for the ESS instruments. Developments here, in parallel to those on the Multi-Blade design, will focus on proving the suitability of such detectors in terms of scattering, dynamic range and stability. These developments are being pushed by a partnership with an in-kind contribution from Milan-Bicocca, CNR and INFN with CERN and ESS in-house effort.

5.2.3 A1-CLD

The A1-CLD prototype [**?**] is a design update in-kind contribution for ESS from HZG/DENEX [**?**] and exploits the neutron conversion in one single layer operated at a very small grazing angle ($<$2.5°) to increase the detection efficiency. The efficiency is quoted to be $\sim$75% at 5Å. Due to the extreme inclined angle, this geometry should offer higher rate capabilities than traditional ^{3}He gaseous devices by a factor of 20–50. There are many mechanical engineering challenges still left to realise this prototype concept as a demonstrated detector geometry, however, it has great potential once these hurdles can be overcome.

5.2.4 ^{3}He detectors

^{3}He detectors have to be excluded for the low angle region of LoKI due to their inability to cope with the rates and spatial resolution required. A ^{3}He-MSGC could possibly match the rate requirements and provide the necessary resolution, however the need for efficient tiling would reduce the active area across the detector.

5.3 High-angle detectors (2°/4°-56°/90°)

The detector options for the two geometries are examined separately:
WINDOW FRAME CONFIGURATION

5.3.1 Multi-Blade

The Multi-Blade detector could be one of the options for both outer panels of the window frame geometry. See subsection 5.2.1.

5.3.2 Micro-Pattern Gaseous Detectors (MPGD)

MPGDs also fulfil the requirements for the high angle detectors. See subsection 5.2.2.

Due to large area coverage scintillators are excluded as an option. Similarly to scintillators, although ^{3}He detectors satisfy the rate and resolution requirements for the outer panels, the large surface area that needs to be covered significantly increases the cost of the instrument and has to be excluded.

A more detailed performance study in combination with a cost analysis will determine the most appropriate technology solution for the window frame.

'BARREL' CONFIGURATION

If the 'barrel' geometry is adopted, it is foreseen to cover the higher angle region with cylindrically arranged detector banks, based on a single-converter layer of ^{10}B. It has been shown that this geometry combines a number of advantages, e.g. high efficiency at low scattering angles of interest and excellent polar angle resolution due to the low incident angle of the incoming neutrons.

At this early stage of the evaluation it is not clear which readout would be better suitable for such a gas detector. One option would be a MWPC. Another could be to go for a GEM-like arrangement. It will depend on the refined resolution requirements, the background caused by rescattered neutrons on the detector material and of course the cost of the whole setup, as defined by the number of readout channels and the respective electronics.

This will require optimization, which needs to be done during phase 2, with advanced simulation tools which are near completion. Specific configurations suggested by the optimized simulations will need experimental verification.

5.3.3 Single ^{10}B-layer MWPC

The possibility to use a MWPC with a single converting layer of boron carbide in back-scattering mode has been evaluated in [**?**]. It presents a lot of attractive features in terms of efficiency and resolution. As the evaluation proceeds more aspects of the design will become clearer, e.g. size, number of readout channels, best option for signal collection, cost.

5.3.4 Single ^{10}B-layer GEM

The same principle with a single converting layer can work with a GEM configuration instead of anode wires. Again a more detailed evaluation needs to be done before making a decision.

Scintillators and ^{3}He detectors cannot be considered because of the large surface area and cost.

6 Readout Electronics

The design of the readout electronics for all the ESS detectors is foreseen to be a collaborative effort with the RAL TD and ISIS. There is a concept in place for both the front-end and the back-end electronics, which is going to be tested and refined as the detector prototypes become larger and closer to the realistic detector size. The effort will be intensified in 2015. The bandwidth is not anticipated to be an issue for this apparatus.

7 In-kind Contributions

Possible in-kind contributors have been identified and contacts with the ESS Detector Group have been established. Figure 7 shows a preliminary picture of the construction possibilities. A dedicated document is in preparation as part of the requested documents for the toll gate 2 decision.

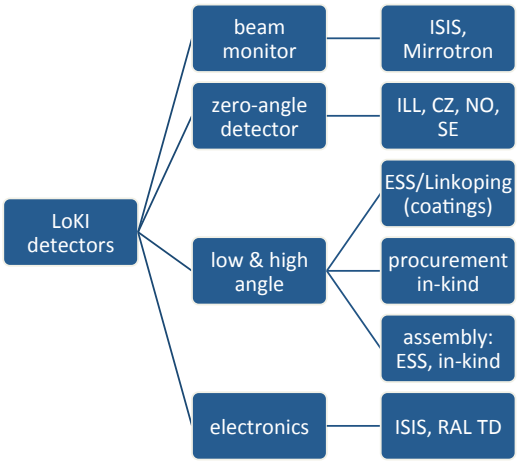

Figure 7: Preliminary in-kind partners for the detector construction phase.

8 Schedule

In the light of these developments which are ongoing, it is important to determine whether they are realistic to be deployed *as tested and mission-ready technologies*. Part of the overall strategy for detectors at ESS, to be able to contribute to the early success strategy of ESS as a whole, is that all detector technologies that are installed on ESS instruments should have been previously demonstrated elsewhere, and not be prototypes, i.e. *no prototypes installed at ESS.*

To determine whether this is realistic for a day 1 SANS instrument, the Multi-Blade detector design is taken as representative of the developments as a whole. This is so as to not over-complicate the picture. The details of the timings of developments differ between the technologies under development, however in terms of steps to be demonstrated, they are the same. At the point where the technology choice needs to be taken for the instrument, the status of all relevant technologies would be reviewed, and the best option chosen.

The schedule for LoKI and the detector developments targeted towards it is shown in Figure 8. The long time scale of the detector developments, which are already underway for the most critical of the options, can be immediately seen from this figure. This underlines the necessity to keep a couple of technology options open, as outlined in the section above, in case of unexpected findings during the detector development process.

With the foreseen developments, it is possible to have fully proven and demonstrated the detector technologies such that they can be chosen in time and built for such an instrument (see Figure 9).

In summary, the schedule for developments looks realistic that detector technology availability should not inhibit the successful operation of LoKI as a day 1 instrument at ESS, contributing to the early success strategy at ESS.

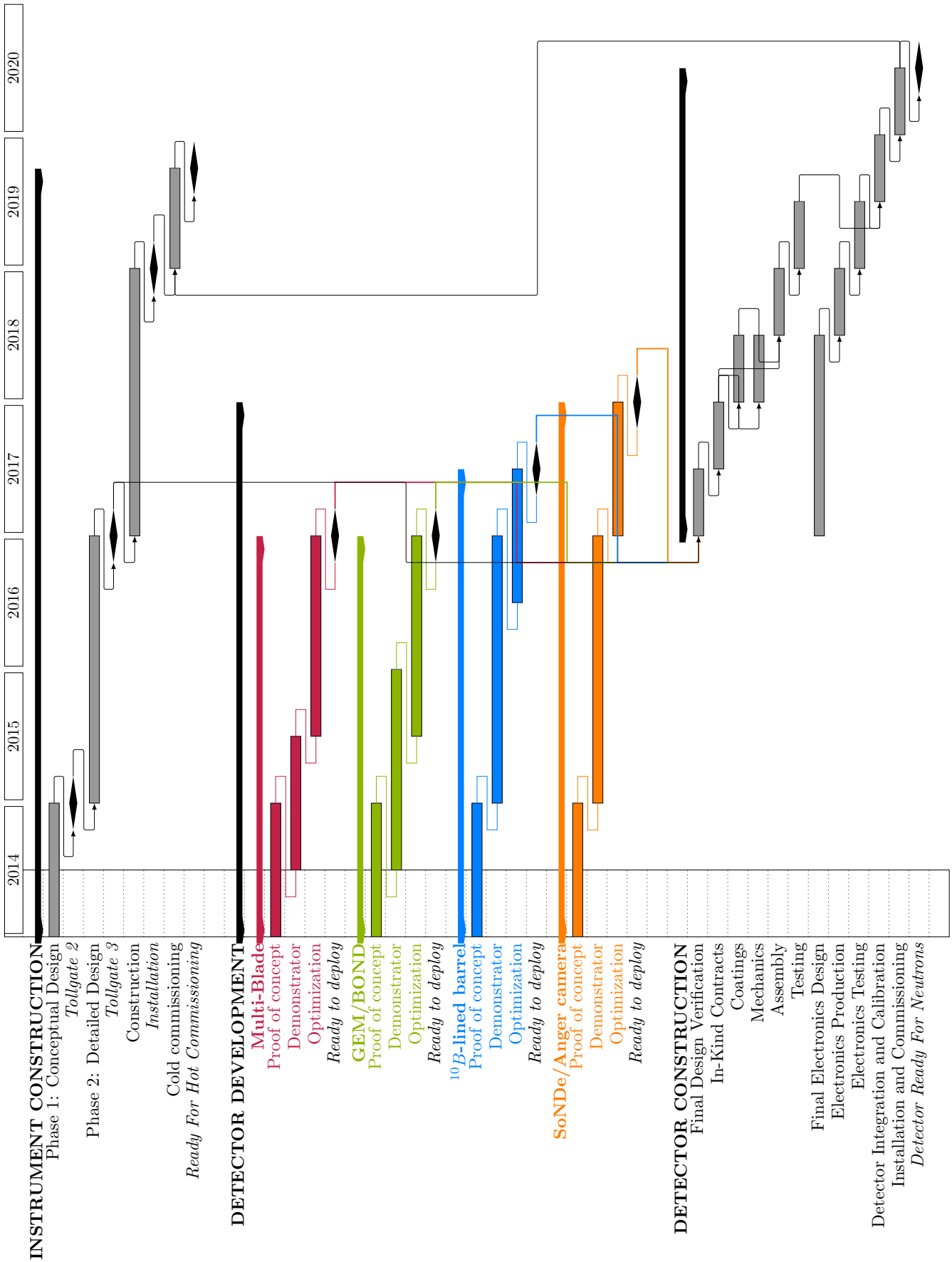

Figure 8: Time schedule for prototyping, construction, assembly and commissioning of the LoKI detectors.

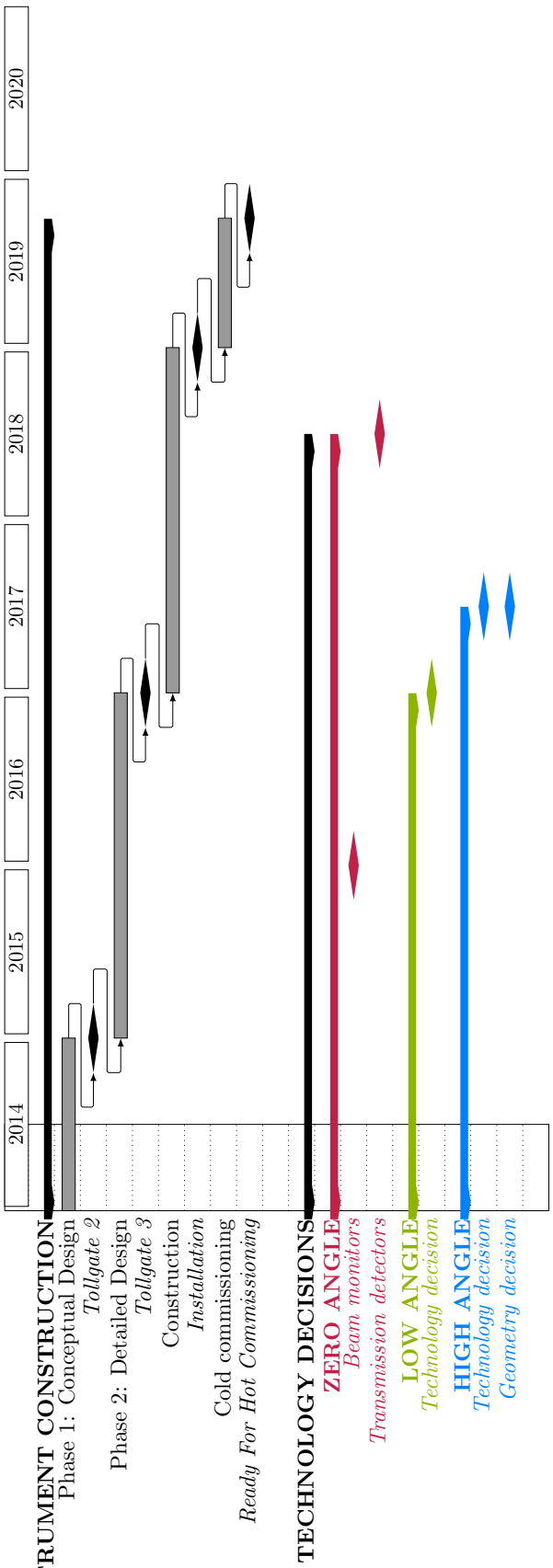

Figure 9: Decision graph with selection points in time for the appropriate technology (and geometry) of the LoKI detectors. Note that the low-angle detector is the key driver for the scientific performance of the instrument.

9 Cost

This section is under development and the price envelopes will be presented in the STAP review.

10 Conclusion (DRAFT)

The requirements for LoKI are outlined and they are presently understood. A review of state of the art detectors is presented in order to give a baseline for 'gold standard' detectors. Options are compared to the requirements, cost, schedule and gold standards. Based on these comparisons, a few options are identified as appropriate for LoKI. These options are laid out in terms of time schedule with explicit decision points for each technology.

Different decision points will come at different times for LoKI detectors due to the different criticality of each angle region. The zero- and low-angle regions are the ones with the most difficult requirements, so the development of the suitable detector technologies needs to be prioritized and an earlier decision in time has to be made. For the high angle detector banks the requirements are looser and the technology decision is less time critical.

Table 3 is an attempt to summarize the current status of technology options with respect to their maturity, cost and requirements.

	spatial resolution	rate capability	cost	maturity
zero-angle				
gaseous detectors	ok	maybe	ok	development
scintillators	ok	maybe	ok	development
semiconductors	ok	ok	maybe	concept
fission chambers	ok	maybe	ok	development
micromegas	ok	ok	ok	concept
low-angle				
Multi-Blade	ok	ok	ok	prototype
MPGD	ok	ok	ok	concept
A1-CLD	ok	maybe	maybe	prototype
scintillators	maybe	maybe	maybe	development
^{3}He	no	no	no	mature
high-angle (WF)				
Multi-Blade	ok	ok	ok	prototype
MPGD	ok	ok	ok	concept
scintillators	ok	ok	no	N/A
^{3}He	ok	ok	no	N/A
high-angle (B)				
MWPC	ok	ok	ok	development
GEM	ok	ok	ok	development
scintillators	ok	ok	no	N/A
^{3}He	ok	ok	no	N/A

Table 3: Detector technology qualification for the 'window frame' and 'barrel' configuration. The rightmost column signifies the maturity of each technology, ranging from 'detector concept' to 'mature'.

A Detector Performance Evaluation

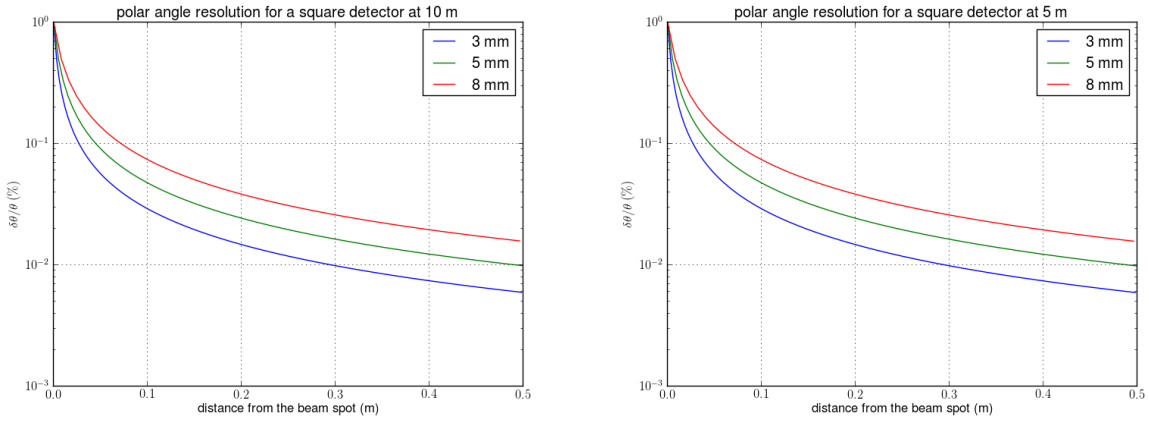

Figure 10: Polar angle resolution for a 1×1 m^2 detector placed at 10 m and 5 m from the sample.

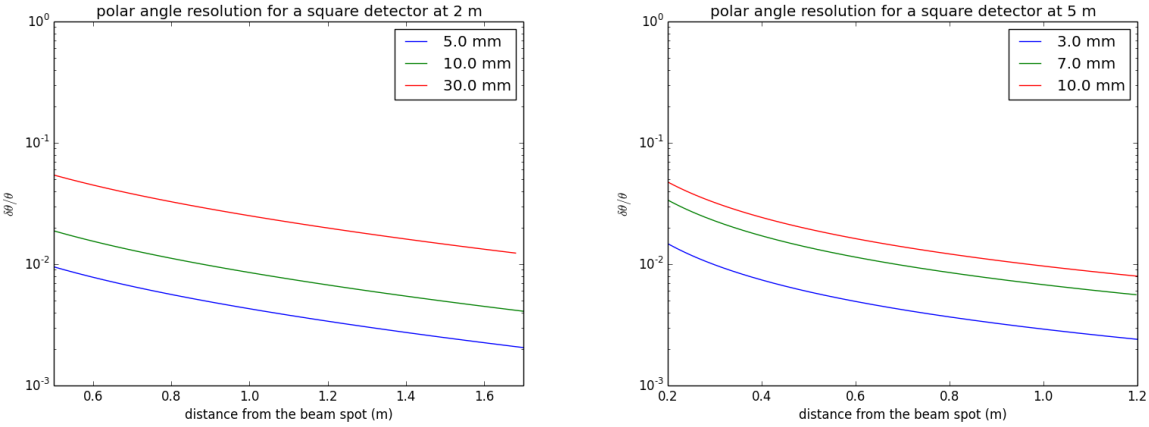

Figure 11: Polar angle resolution for the 2 WF panels with the hole in the middle.

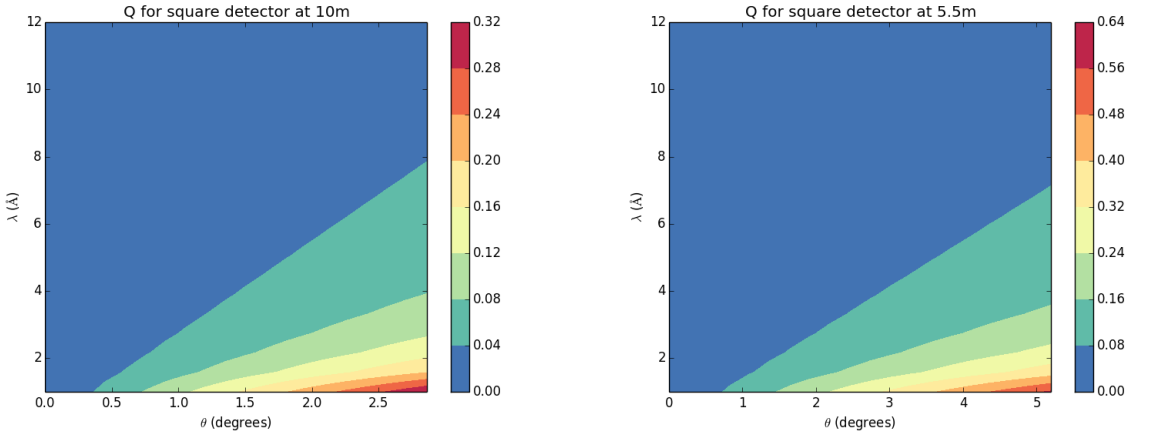

Figure 12: Q access for a 1×1 m^2 detector placed at 10 m and 5.5 m from the sample (for flat θ and λ distributions).

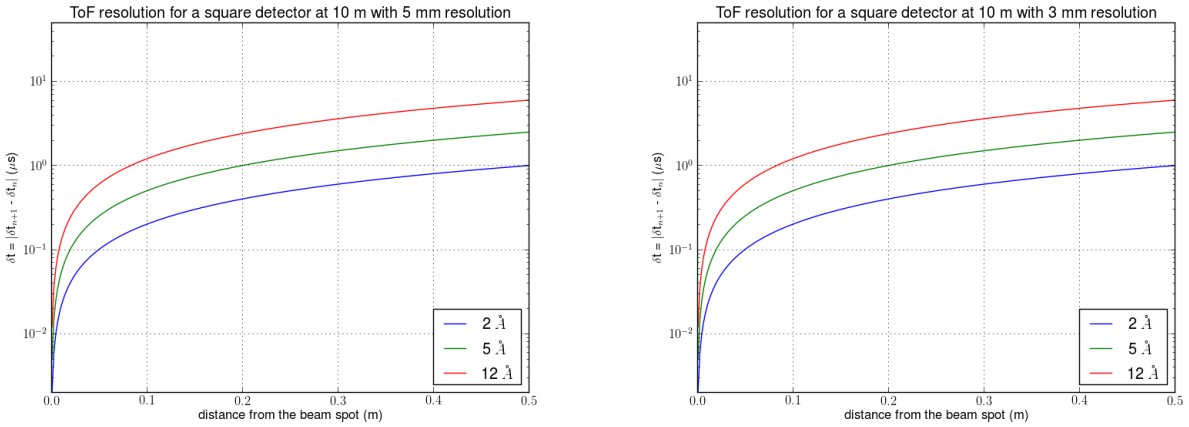

(a) (b)

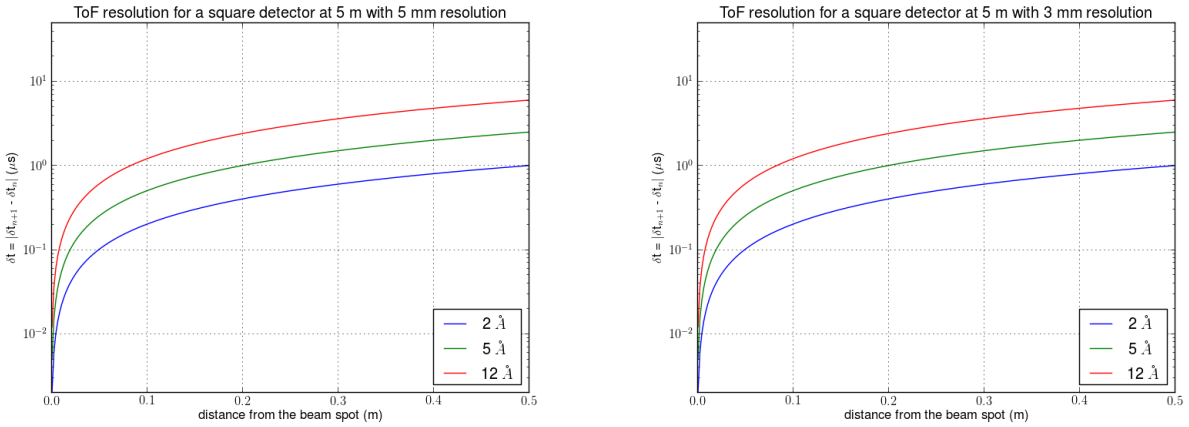

(c) (d)

Figure 13: ToF absolute resolutions for a 1×1 m^2 detector placed at 10 m and 5.5 m from the sample and two different spatial resolutions.

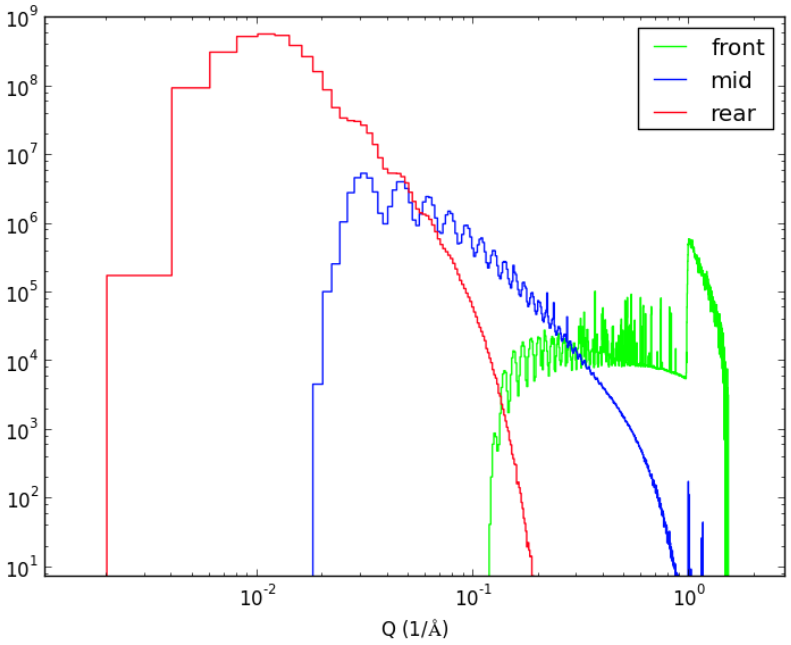

Figure 14: Q distribution for spherical structures of 200 Åradius (2 m collimation).

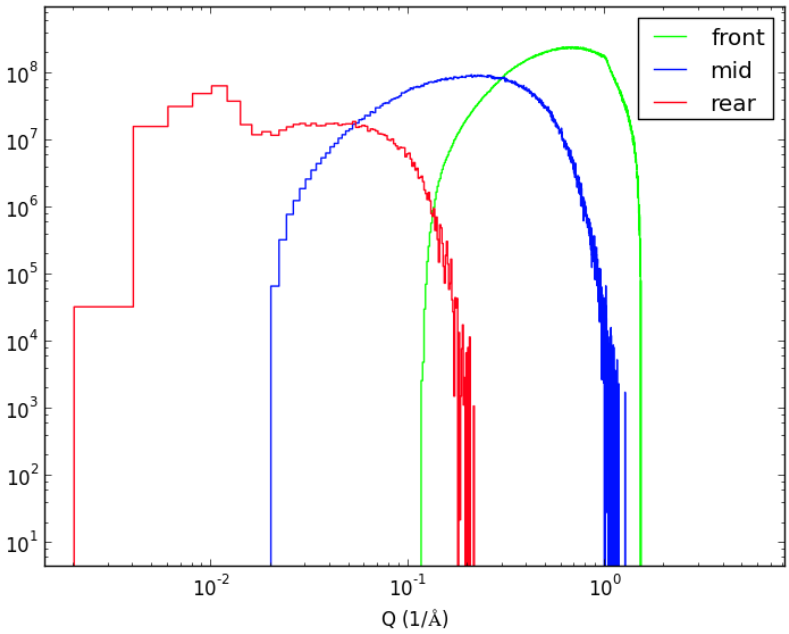

Figure 15: Q distribution for water sample (2 m collimation).

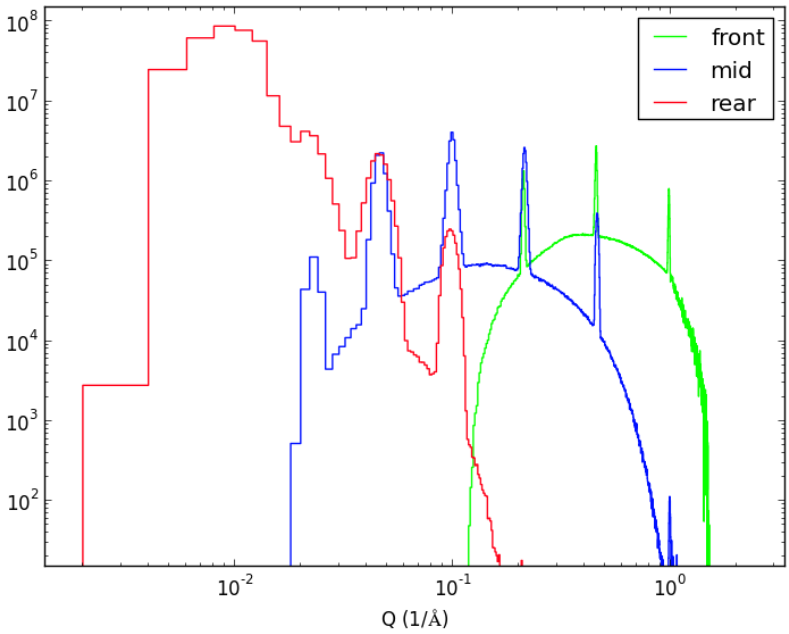

Figure 16: Logarithmically spaced peaks to demonstrate the impact of the instrument resolution on Q. Detector resolution is not included.

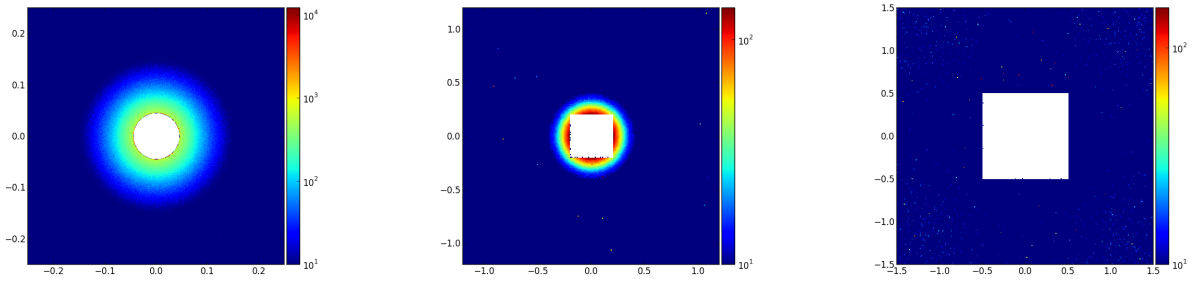

(a) (b) (c)

Figure 17: XY hit distribution on the window frame detectors for 200 Å spheres and 2 m collimation. The bin size of the rear detector is 1 mm^2. For the other two panels it is 1 cm^2.

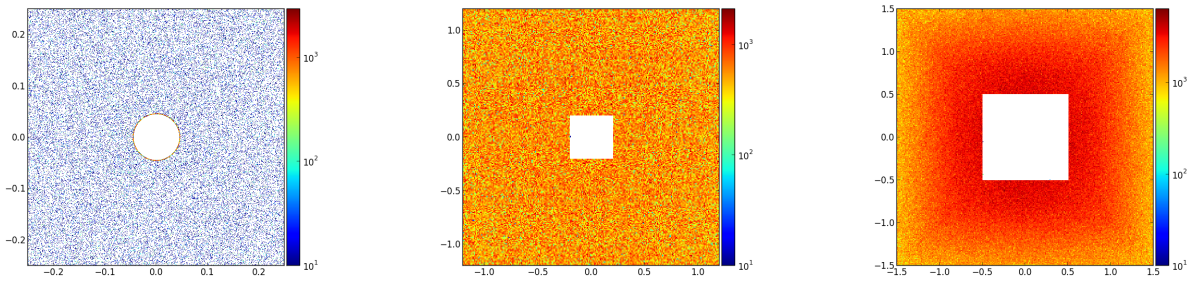

(a) (b) (c)

Figure 18: XY hit distribution on the window frame detectors for a water sample and 2 m collimation. The bin size of the rear detector is 1 mm^2. For the other two panels it is 1 cm^2.

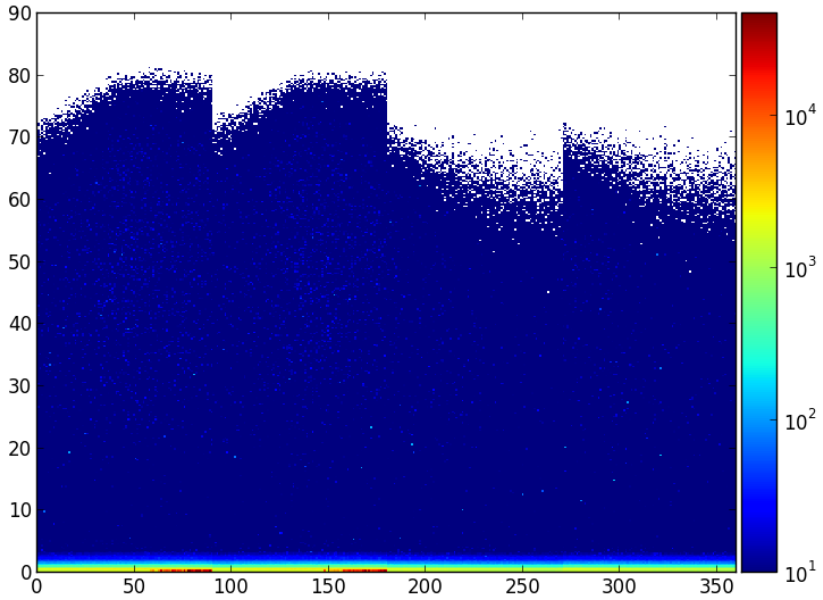

Figure 19: 'Barrel' $\theta - \phi$ distrubution for the 200 Å spheres.

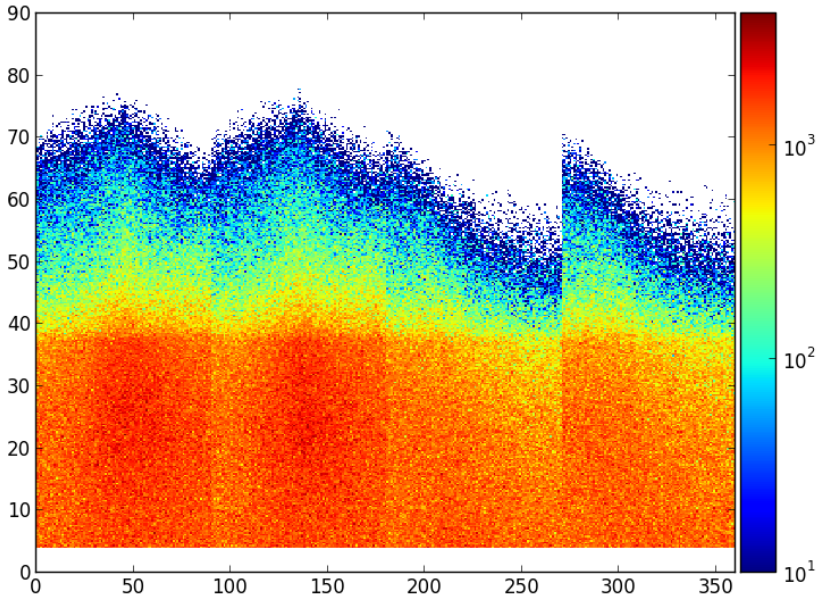

Figure 20: 'Barrel' $\theta - \phi$ distrubution for the water sample.